Well-Dispersed NiS Nanoparticles Grown on Functionalized CoS Nanospheres Surface as a high performance Counter Electrode for Quantum Dot-Sensitized Solar Cells

Hee-Je Kim, Hyun-Dong Lee, S. Srinivasa Rao, Araveeti Eswar Reddy, Soo-Kyoung Kim, Chebrolu Venkata Thulasi-Varma*

School of Electrical Engineering, Pusan National University, Gumjeong-Ku, Jangjeong-Dong, Busan 609-735, South Korea

*Corresponding author. Tel.: +82 10 4675 2989; fax.: +82 51 510 2364;

E-mail address: tulasinaidunaidu@gmail.com

Dark current-Voltage characteristics of QDSSCs with CoS-NiS, CoS and Pt CEs:

The dark current-voltage characteristics of QDSSCs with CoS, CoNiS, and Pt CEs are shown in Fig S1. It provides further insight into the changes occurring during the deposition temperature process. In the dark under forward bias, electrons enter into the TiO_2 cell and react with S^{2-}_X, which means the S^{2-} ions are reduced, and the resultant S^{2-} is oxidized to S^{2-}_X at the CE. This information can be used to estimate the charge recombination at the interface between the CE/polysulfide electrolyte interfaces. On the other hand, the CoS-NiS CE presents low dark current in comparison with CoS and Pt CEs, which means the CoS-NiS CE has good adherence to the FTO substrate and is robust with better catalytic features in the QDSSCs.

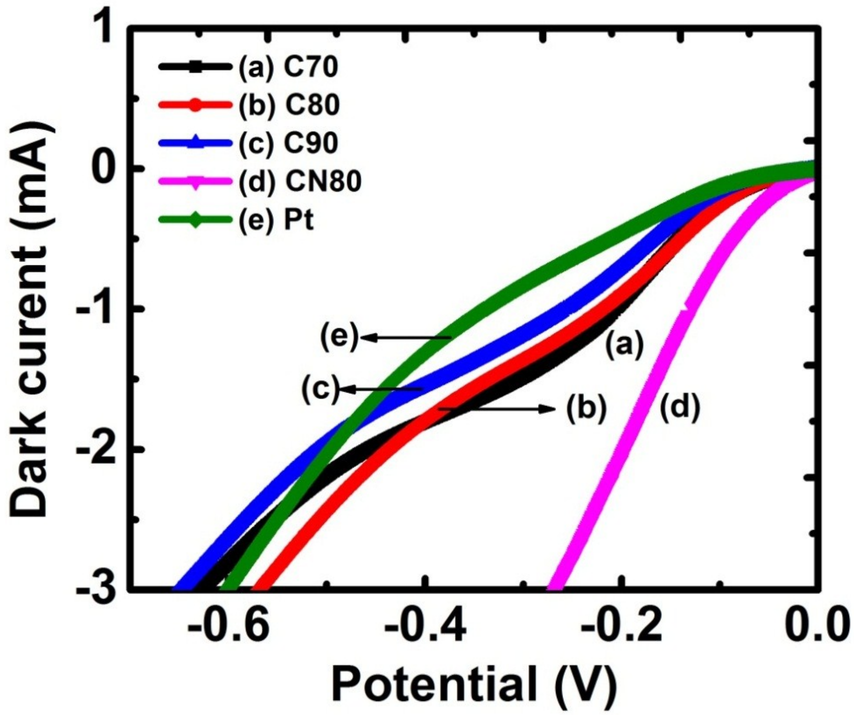

Fig. S1 Dark current Vs potential curves of QDSSCs with CoS-NiS, CoS, and Pt CEs under dark condition.

Effect of composite CoS-NiS (CN80), and CoS (C70, C80, and C90) CEs thickness on performance of the QDSSCs

To further understand the dependence of short-circuit current density and fill factor on the thickness of CoS-NiS, and CoS CEs, electrochemical impedance spectroscopy was also used to characterize the quantum-dot sensitized solar cells. Four cells fabricated from CoS-NiS, and CoS CEs with thicknesses of 789 nm, 848 nm, 750 nm, and 873 nm are shown in Fig S2. Obviously, the decreased first semicircle in Fig indicates the acceleration of the electron transfer at the CE/polysulfide electrolyte interface. This is consistent with the enhanced fill factor due to decreased series resistance in the CoS-NiS CE when compared to CoS (C70, C80, and C90), and Pt CEs.

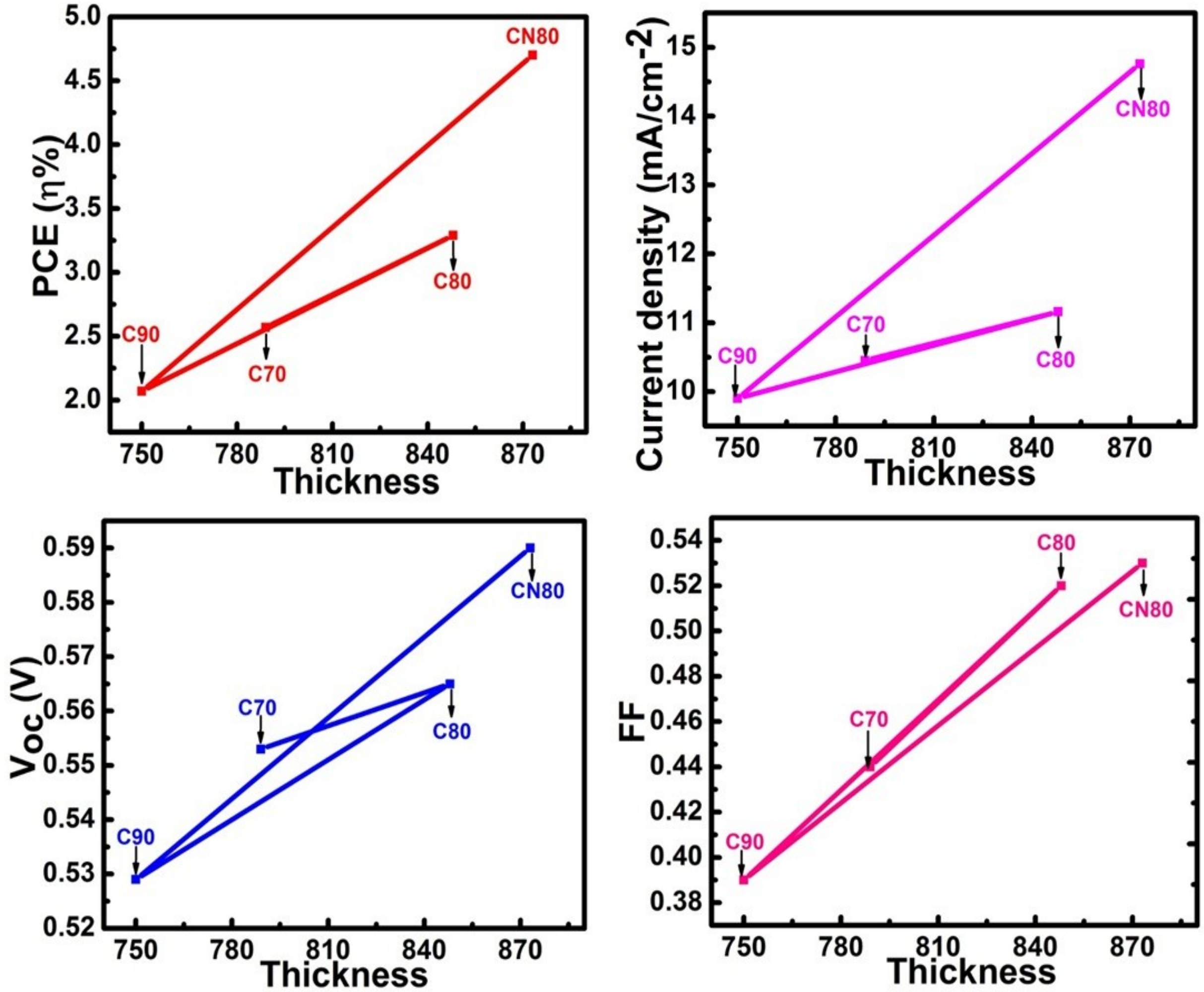

Fig. S2 Parameters of the quantum dot-sensitized solar cell using with different thickness as counter electrodes measured under AM 1.5 illumination. (a) Dependence of the energy conversion efficiency on film thickness. (b) Dependence of the current density on film thickness. (c) Dependence of the open-circuit voltage on film thickness. (d) Dependence of the fill factor on film thickness.

It was also observed that the 789 nm thickness of CoS (C70) CE deposited on FTO substrate is constructed with small nanoparticle size of 0.5 nm, as shown in the inset Fig 2(a, a1) when the film thickness is increased to 848 nm, the size of nanoparticles grew into nanospheres. Moreover, the film thickness was also increased 0.5 to 2 nm (Fig 2(b, b1). Further increase in the thickness was not observed when the deposition temperature was increased over 90^{o}. This means the nanospheres surface microstructure disappeared and an uneven CoS was formed on the FTO substrate, as shown in the Fig 2(C, and C1). In fact we found that the energy conversion efficiency could be greatly improved with a composite CoS-NiS CE in comparison with binary CoS CEs. In addition, the conversion efficiency could be also greatly improved by increasing current density. It can be concluded from the thickness of composite CoS-NiS CE, the nanoparticle size of CoS-NiS gradually increased through agglomeration and their porosity declined with controlling the deposition temperature. This is mainly due to the aggregation of the nanoparticles during deposition temperature.

Effect of composite CoS-NiS, and CoS CEs film thickness on sheet resistance:

The variation of sheet resistance of CoS-NiS and CoS CEs with the film thickness is clearly depicted in Fig S4. The sheet resistance (R_s) of the composite CoS-NiS CE decreased with controlling the deposition temperature and the film thickness increased respectively. The thickness range between 789 to 873 nm. According to the SEM micrographs, CoS-NiS CE has uniform surface morphology and good quality over the entire FTO substrate without any empty surface regions. Moreover, when the deposition time exceeded 80^{o}, the nanoparticle surface microstructure disappeared and an uneven CoS was formed on the FTO substrate. [It is clear evidence from the Fig 2(C and C1)]. These results indicates that the conductivity of the CoS-NiS CE can be improved, which results higher current density and fill factor. These factors will clearly effecting on the performance of QDSSCs.

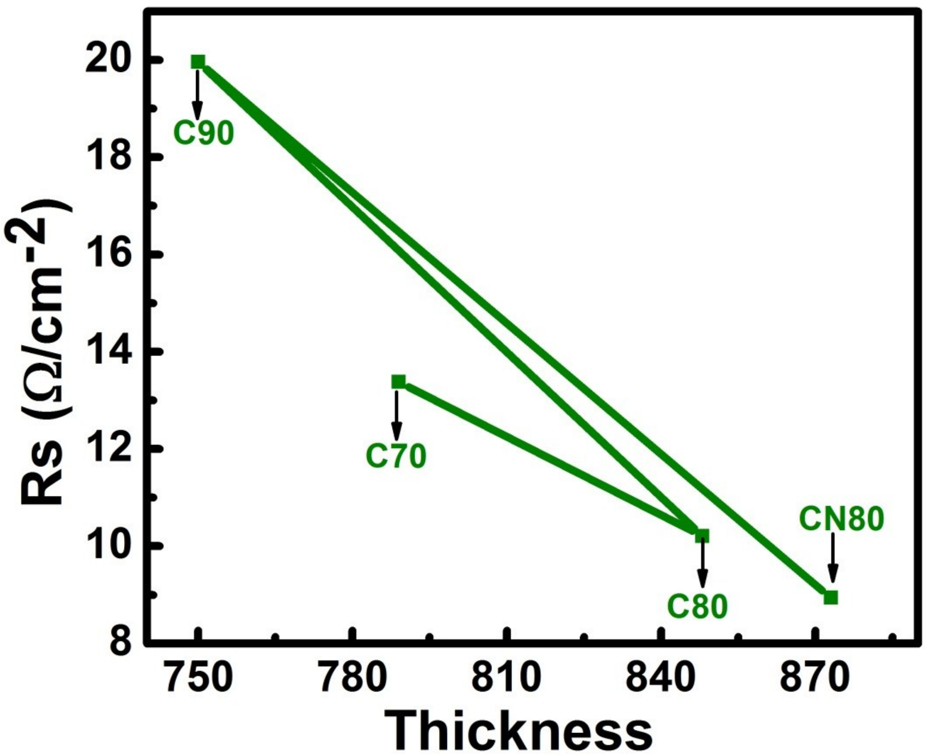

Fig. S3 The dependence of sheet resistance of CoS-NiS (CN80) and CoS (C70, C80, and C90) CEs on film thickness.

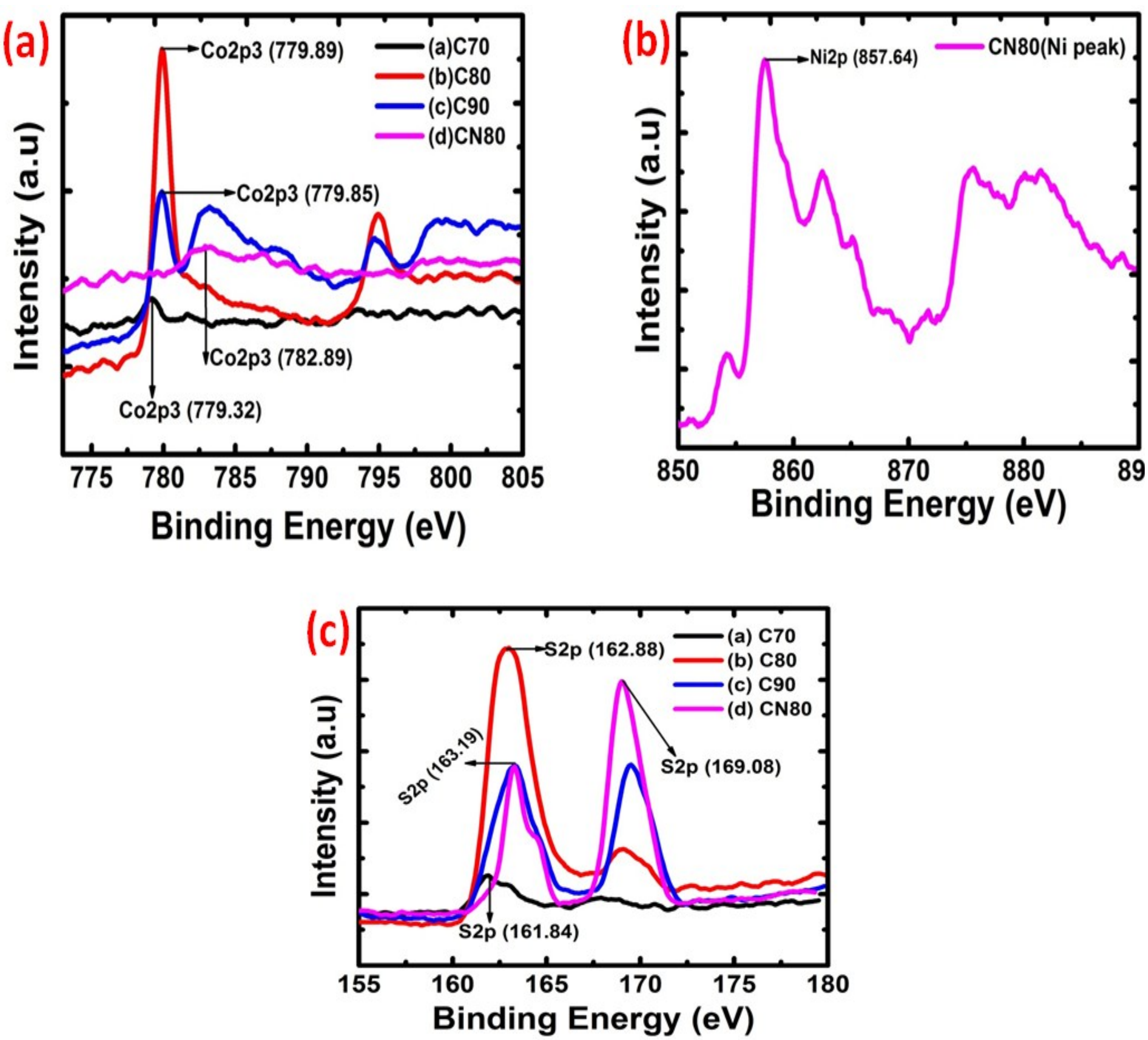

Fig. S4 (a) Co2p$_3$ spectra of CoS (C70, C80, and C90), and CoS-NiS (CN80) CEs (b) Ni2p spectra of CoS-NiS CE, (c) S2p spectra of CoS (C70, C80, and C90), and CoS-NiS (CN80) CEs.

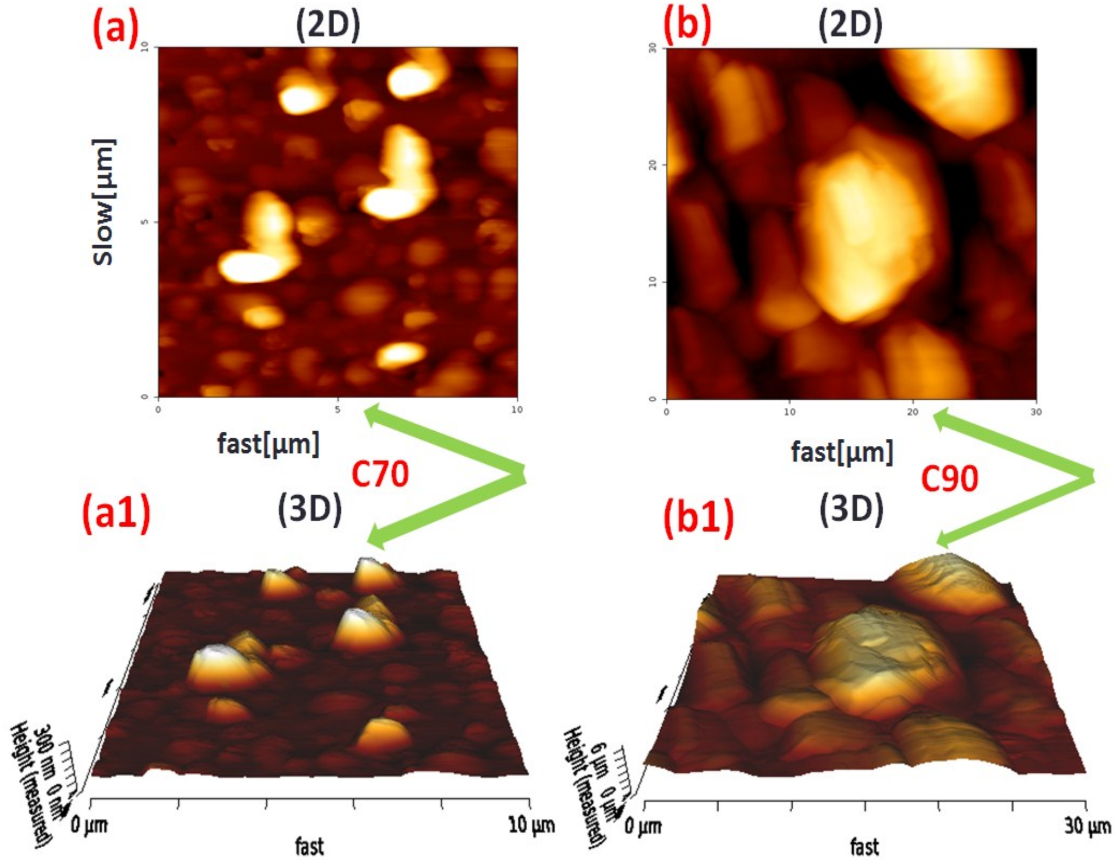

Fig. S5 2D (a, b) and 3D (a1, b1) AFM images of CoS (C70, and C90) CEs respectively.